Cramér-Rao Lower Bound Analysis of Differential Signal Strength Fingerprinting for Crowdsourced IoT Localization

Jiseon Moon, Christos Laoudias, Ran Guan, Sunwoo Kim, *Senior Member, IEEE*, Demetrios Zeinalipour-Yazti, *Senior Member, IEEE*, and Christos G. Panayiotou

***Abstract*—Crowdsourcing is considered an efficient and promising paradigm for constructing large-scale signal fingerprint radio maps due to the proliferation of Wi-Fi-enabled devices. However, a crowdsourced Indoor Positioning System (IPS) has to handle diverse devices and the inherent heterogeneity in Received Signal Strength (RSS) measurements. To address the device heterogeneity problem, differential fingerprinting methods have been explored, which mitigate the device characteristics that cause RSS from different commercial devices to report differently. In this paper, we focus on Mean Differential Fingerprinting (MDF) that produces the differential fingerprints by subtracting the mean RSS value of all APs from the original RSS fingerprints. We study the localization performance of the MDF method by means of the Cramér-Rao Lower Bound (CRLB) and show analytically that it outperforms another method that addresses device diversity. Furthermore, we evaluate the localization accuracy of existing solutions using real-life Wi-Fi RSS datasets collected by multiple consumer devices. The experimental results confirm our analytical findings and demonstrate the effectiveness of the MDF method to mitigate device diversity, as well as other factors that affect the RSS readings including the device carrying mode and power control schemes of the Wi-Fi infrastructure, thus contributing to the wider adoption of crowdsourced IPS.**

***Index Terms*—Indoor localization, Differential Signal Strength Fingerprinting, Device Heterogeneity, Cramér-Rao Lower Bound**

I. Introduction

RECENTLY, Location-Based Services (LBS) have been rapidly growing due to the demand for location and navigation-related applications [1] in health care [2, 3], advertisement [4], autonomous vehicle systems [5], and smart cities [6]. Global Navigation Satellite Systems (GNSS) are the de facto localization technology for outdoor applications [7]; however, to date there is not a single prevailing positioning solution in GNSS-deprived environments such as urban canyons and indoor spaces.

Fingerprinting wireless signals such as Received Signal Strength (RSS) has become an attractive solution for the deployment of Indoor Positioning Systems (IPS). This is mainly due to the explosive growth of Wi-Fi Access Points (AP) and the proliferation of Wi-Fi-enabled IoT devices including smartphones [8]. Such IoT devices are equipped with various types of sensors and can be readily used to perform various crowdsourcing/crowdsensing tasks in a collaborative fashion, e.g., estimating air temperature [9]. Smartphones and other IoT devices can be also utilized to recognize the spatial characteristics of the localization area by sensing the signal fingerprints required for deploying IPS [10–12]. Typically, a signal fingerprint refers to the set of RSS values collected from surrounding Wi-Fi APs. Prior to positioning, the fingerprinting system constructs a RSS radio map of the area of interest based on the fingerprints annotated with location tags. When it comes to positioning, the unknown user location is estimated by matching the observed fingerprint to a fingerprint stored in the radio map. Although fingerprinting localization has comparable or even better localization performance than other solutions without the cost of additional hardware or infrastructure, it has not yet been widely adopted in real-life application scenarios. The main limitation of fingerprinting localization is that it requires time-consuming and labor-intensive measurement campaigns to build and maintain the RSS radio map.

To this end, crowdsourcing has recently emerged as a viable alternative to relieve the burden of fingerprint data collection by leveraging Wi-Fi RSS readings shared by users participating voluntarily [13–15]. These volunteers record Wi-Fi RSS readings using their own IoT devices such as smartphones and tablets, while moving within the area of interest, and then share the collected fingerprints.

Crowdsourcing, however, introduces additional challenges to fingerprinting IPS. Besides the need to engage users for contributing their collected RSS data through the provision of incentives [16], crowdsourcing raises some new technical issues. For instance, a major problem is that a device used to collect data for the radio map usually is not the same as the user-carried device to be positioned when the system operates, i.e., the *device diversity* or *device heterogeneity* problem.

This work was supported by Institute of Information & communications Technology Planning & Evaluation (IITP) grant funded by the Korea government (NFA) (No.2019-0-01325, Developed of wireless communication tracking based location information system in disaster scene for fire-fighters and person who requested rescue) *(corresponding author: Sunwoo Kim)*

The work of Christos Laoudias is supported by the European Union's Horizon 2020 research and innovation programme under grant agreement No 739551 (KIOS CoE) and from the Republic of Cyprus through the Deputy Ministry of Research, Innovation and Digital Policy.

Jiseon Moon and Sunwoo Kim are with the Department of Electronic Engineering, Hanyang University, Seoul 04763, South Korea (e-mail: jiseonmoon@hanyang.ac.kr; remero@hanyang.ac.kr).

Christos Laoudias and Christos G. Panayiotou are with the KIOS Research and Innovation Center of Excellence, University of Cyprus, Nicosia, Cyprus (e-mail: laoudias@ucy.ac.cy; christosp@ucy.ac.cy).

Ran Guan is with the Riemann Laboratory, Huawei Technologies, Shenzhen, China. (e-mail: guanran@huawei.com).

Demetrios Zeinalipour-Yazti is with the Department of Computer Science, University of Cyprus, Nicosia, Cyprus (e-mail: dzeina@cs.ucy.ac.cy).

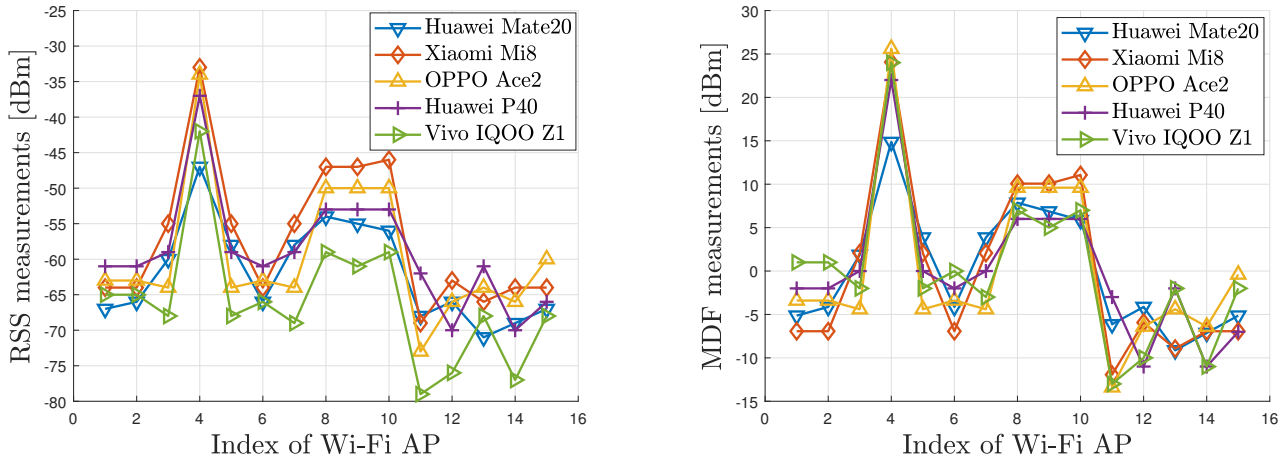

Fig. 1: Fingerprint measurements collected by heterogeneous devices from several Wi-Fi APs. (a) RSS data. (b) MDF data.

Notice that the reported RSS measurements can be affected by factors that are related to multi-vendor device characteristics, such as Wi-Fi chipset, antenna design, device packaging, operating system software stack, etc. Figure 1a shows the RSS fingerprints collected at the same position via five smartphones with different Wi-Fi chipsets. The fingerprints deviation can be observed visually, where raw RSS measurements can lead to a significant deviation up to 17 dBm. This is not compatible to generate radio maps and can cause high localization errors in the crowdsourced system. As it is hard to quantify how these factors affect RSS measurements, they are collectively referred to as device heterogeneity in this work. Little has been done to investigate how device heterogeneity ripples through and ultimately affects positioning performance. It is intuitive, however, that the larger the device heterogeneity is, the less valuable the radio maps are for a new device to be positioned, thus limiting the applicability and wider acceptance of fingerprinting IPS.

Beyond device heterogeneity, there are additional factors that may impact RSS measurements and introduce high location errors in real-life fingerprinting IPS. For instance, even if two users carry exactly the same device they may be facing different directions when they collect data at the same location. In this case, a user may be blocking the signals from an AP received by the device, while the other user may not. As the human body leads to additional signal attenuation when a user is standing between the transmitter (i.e., the Wi-Fi AP) and the receiver (i.e., the user's device), a bias is introduced in the RSS measurements collected by one user, but not the other, which is known as *body-loss* impact [17]. Even when these two users are facing the same direction they may carry their devices in a different way, e.g., hand-held with different device orientations (e.g., horizontal or vertical) that may be blocking fully or partially the device's antenna leading to the *hand-grip* impact [17], or inside bag, backpack, pocket, etc., i.e., *carrying mode* [18]. In these cases, different bias values are introduced in the RSS readings. Finally, Wi-Fi APs may come with dynamic transmit *power control* capabilities, also known as cell breathing for network operation reasons [19]. In fact, many commercially available Wi-Fi APs automatically adjust their transmit power and working channel based on interference from authorized APs, rogue APs, and non-Wi-Fi interference sources to make the network operate at the optimal performance [20]. Due to this functionality, two users carrying exactly the same device in exactly the same way may report significantly different RSS values if they visit the same location at different times during the day, when a different power control policy is in place. In this work, we treat these impacts using techniques proposed mainly to address device heterogeneity.

How to mitigate device heterogeneity remains an active research topic and existing solutions can be broadly categorised into two approaches, namely the *calibration* and the *calibration-free* schemes. Earlier crowdsourcing system, including *Molé* [21] adopts the calibration scheme and calibrates RSS values collected by heterogeneous devices at the same known location by applying linear fitting. This approach, however, requires perfectly aligned fingerprint pairs from a large number of devices, rendering it impractical in many applications. As a result, the calibration-free scheme attracts more attention as it employs data transformation techniques to remove device-dependent characteristics from the RSS readings, rather than perfectly aligned fingerprint pairs from multiple devices.

For example, the *FreeLoc* system generates relative RSS values at a particular location in a manner similar to Rank Based Fingerprinting (RBF) [22], which sorts the Wi-Fi APs from the strongest to the weakest by RSS values. Similarly, the Hyperbolic Location Fingerprinting (HLF) [23] uses normalized logarithm RSS ratios for all AP pairs in the observed fingerprint. The first method for differential fingerprinting, named DIFF, constructs fingerprints by taking the RSS differences between all possible AP pairs [24]. Many variants are also proposed, including the Signal Strength Differences (SSD) method that subtracts the RSS value of an anchor AP from the other RSS values of the original fingerprints [25]. In [26], it is

demonstrated that the DIFF method achieves better accuracy than SSD when diverse devices are considered. The Mean Differential Fingerprint (MDF) method is another variant, which subtracts the mean RSS of all APs from the original fingerprint [27]. Although some recent applications have been proposed for existing differential fingerprints [28, 29], there are no studies investigating their expected performance in a theoretical way.

In our previous work, we assessed the performance of differential fingerprinting methods, including the proposed MDF approach, by means of analytical models for the probability of correct location estimation and conducted experiments with Wi-Fi RSS datasets collected in small-scale setups [30]. In this paper, we perform a rigorous theoretical analysis and comparison of differential fingerprinting methods by means of the Cramér-Rao Lower Bound (CRLB). In particular, we first derive the CRLB of MDF and the existing fingerprinting method in a crowd-sourcing environment with multiple heterogeneous devices. The CRLB is used in estimation theory to derive a lower bound of the variance of an unbiased estimator. In the analysis of IPS, the CRLB denotes that the localization error at a specific position is greater than or equal to X meters given parameters such as the number and the geometry of the APs, as well as the statistical characteristics of the measurements (e.g., noise profile). We employ the CRLB to analyze the performance of various differential fingerprinting methods and demonstrate both analytically and experimentally that the proposed MDF approach outperforms existing solutions.

To this end, the contribution of this work is three-fold:

- The theoretical localization performance in the presence of multiple crowdsourcing devices has not been considered. We first derive the CRLB of the MDF method for crowdsourced fingerprinting systems to assess its performance in terms of localization accuracy. In addition, we extend the existing CRLB derivation for the SSD method to accommodate the presence of multiple heterogeneous devices.
- We employ the CRLB formulations to study the behavior of the MDF and the SSD methods with respect to various system parameters. Our extensive analysis based on the CRLB offers insights about the expected performance of these methods in practice.
- We conduct a thorough experimental evaluation to confirm the theoretical findings. In particular, we use two Wi-Fi RSS datasets collected in real-life indoor environments with multiple devices. We report accuracy results in crowdsourced fingerprinting systems in the presence of device heterogeneity and other factors, e.g., carrying mode and power control, that impact the RSS measurements.

The rest of the paper is structured as follows. Section II overviews crowdsourced fingerprinting localization and outlines differential fingerprinting methods. Section III presents the CRLB for the MDF method and analyzes the theoretical localization performance with respect to various parameters. Section IV presents experimental results and comparison with existing solutions in our performance evaluation. Finally, Section V provides concluding remarks and future work.

II. Overview of Crowdsourced Fingerprinting Localization

This section first provides the background of crowdsourced fingerprinting localization systems. We then review two main differential fingerprinting methods (proposed in [25] and [27]) for mitigating device heterogeneity in crowdsourced systems.

A. Basics of Crowdsourced Localization

Looking at Friis free-space transmission formula $P_r = P_t A_r A_t (d\lambda)^{-2}$, we observe that the received power P_r depends on the transmit power P_t, the effective aperture area of the receiving and transmitting antennas A_r and A_t, the distance d between the antennas and the wavelength of the radio frequency λ. Thus, the RSS value r (in dBm) can be modeled using the simple log-distance radio propagation model

$$r = A - 10\beta \log_{10} d + X, \tag{1}$$

where d is the distance between a device and a Wi-Fi AP, the coefficient β is the path-loss exponent that depends on the propagation conditions (e.g., $\beta = 2$ in open space environments and increases in obstructed indoor spaces), and $X \sim \mathcal{N}(0, \sigma^2)$ is Gaussian noise that disturbs the RSS values, and is also known as shadowing [31]. The term A provides the RSS value at a distance $d = 1\,\mathrm{m}$ and encapsulates device-specific characteristics, such as the antenna gain and transmitter power, etc.

Typically, heterogeneous devices have diverse characteristics leading to different A values. Thus, various devices will report different RSS values, even if they are placed at the same location (i.e., with a fixed distance to a specific Wi-Fi AP). Consequently, reported accuracy with single device and lab conditions can hardly be reproduced in crowdsourced systems, where the user-carried devices are from several manufacturers. Several studies have demonstrated experimentally that a pair of RSS values collected by heterogeneous devices has a linear relation [32, 33]. In other words, the RSS value collected by device m with respect to a reference device can be represented by

$$r^{(m)} = \alpha_{1,m} r^{(1)} + \gamma_{1,m}, \tag{2}$$

where $\alpha_{1,m}$, $\gamma_{1,m}$ are the linear coefficients for mapping the RSS values between devices 1 and m.

Traditional fingerprinting systems consist of two stages, i.e., the *offline* (training) phase and the *online* (positioning) phase. In the *offline* phase, the indoor radio map is generated by exploiting the Wi-Fi RSS value collected at a set of predefined reference positions $\{\mathcal{L} : \ell_i = (x_i, y_i),\ i = 1, \ldots, l\}$. A set of crowdsourcing devices $\{\mathcal{D} : D^{(m)},\ m = 1, \ldots, M\}$ collect RSS values from n Wi-Fi APs. Device $D^{(m)}$ visits a subset of the reference positions $\{\mathcal{L}^{(m)} : \ell_i = (x_i, y_i),\ i = 1, \ldots, l^{(m)}\}$, so that $\mathcal{L}^{(m)} \subseteq \mathcal{L}$ and $\mathcal{L} = \bigcup_{m=1}^{M} \mathcal{L}^{(m)}$. A reference fingerprint $\mathbf{r}_i^{(m)} = [r_{i1}^{(m)}, \ldots, r_{in}^{(m)}]^\top$ associated with location ℓ_i is a vector of RSS readings observed at that location

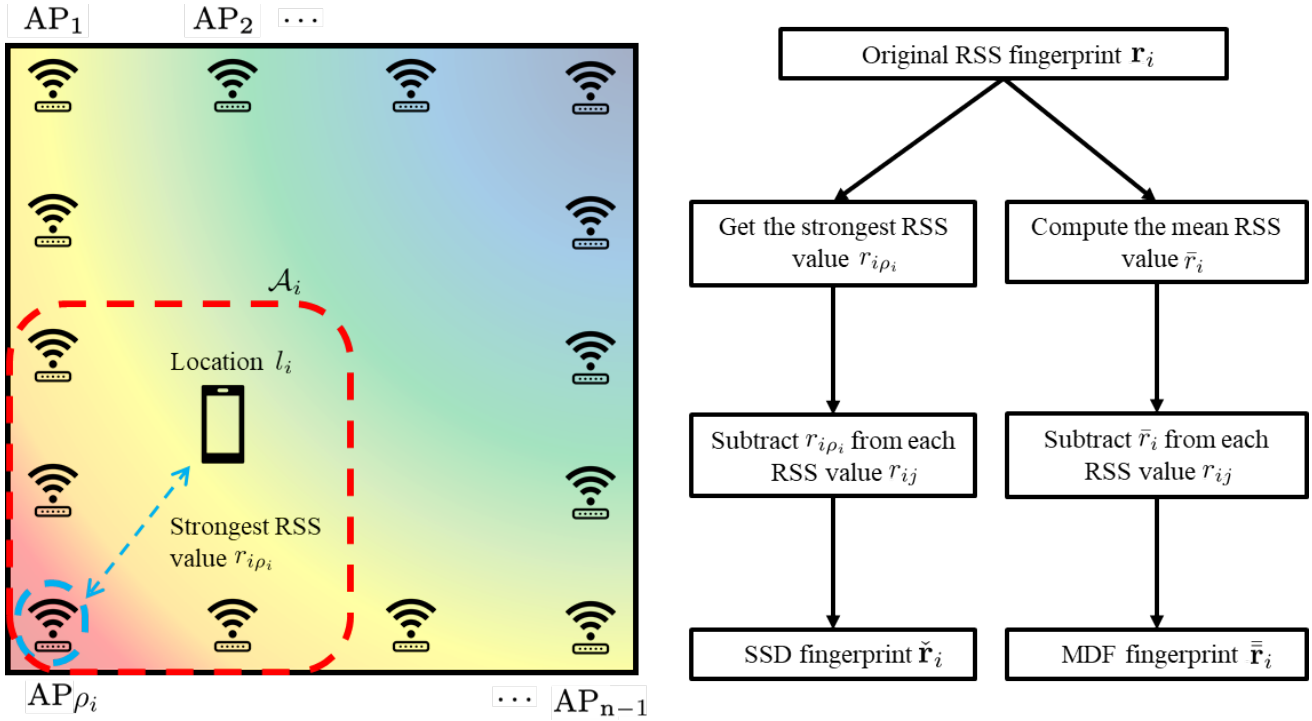

Fig. 2: Generation processes of the differential fingerprints using SSD (cyan) and MDF (red).

and $r_{ij}^{(m)}$ denotes the RSS reading from the j-th AP recorded by device $D^{(m)}$.

Using all available RSS measurements from multiple devices, one can build the crowdsourced RSS radio map $\mathbf{R} \in \bar{\mathbb{Z}}_{l\times n}$ by aggregating the RSS values for each AP across all contributing devices M_i at location ℓ_i, where $1 \leq M_i \leq M$, according to

$$r_{ij} = \frac{1}{M_i} \sum_{m=1}^{M_i} r_{ij}^{(m)}. \tag{3}$$

In the *online* phase, the RSS values collected by the user's device are compared to the radio map created in the offline phase to identify his/her location. Given a new fingerprint $\mathbf{s} = [s_1, \ldots, s_n]^\top$ measured at the unknown location ℓ by the user-carried device $D^{(m')}$, the crowdsourced radio map $\mathbf{R}$ is employed to estimate $\widehat{\ell}$. For simplicity, in this work, we use the K-Nearest Neighbor (K-NN) localization method that determines location as

$$\widehat{\ell}(\mathbf{s}) = \Big(\frac{1}{K}\sum_{o=1}^{K} x_o, \frac{1}{K}\sum_{o=1}^{K} y_o\Big), \tag{4}$$

where (x_o, y_o), $o = 1 \ldots, l$ denote the coordinates of the locations *ordered* according to increasing distance between the reference fingerprints $\mathbf{r}_i$ and the observed fingerprint $\mathbf{s}$, which is computed by

$$D_i^2 = \sum_{j=1}^{n} \big(r_{ij} - s_j\big)^2. \tag{5}$$

Essentially, location is estimated as the mean of the K reference locations with the shortest distances between $\mathbf{r}_i$ and $\mathbf{s}$ in the n-dimensional RSS space. Note that the MDF method is applicable directly to other localization methods including probabilistic approaches.

B. Differential Fingerprinting Methods

The RSS fingerprints are not robust to device diversity because they contain the device-specific term A of each crowdsourcing device; see Appendix C. The main idea of differential fingerprinting methods is to remove A in Eqn. (1). Removing this term representing the device's characteristics makes the differential fingerprints from heterogeneous devices compatible with each other and ultimately enables the creation of crowdsourced radio maps. We present two differential fingerprint methods, namely the SSD [25] and the MDF [27]. For instance, the MDF method smooths differences between devices and shows higher consistency across devices (Fig. 1b), compared to the original RSS measurements (Fig. 1a).

example

1) SSD Fingerprints: In the SSD method, the RSS value of an anchor AP is subtracted from the other RSS values in the original fingerprint in order to create the differential fingerprints [25, 34]. These works consider only small-scale setups, where all Wi-Fi APs are detected in the whole area. Thus, a specific AP was selected a priori to be the anchor AP, e.g., the AP that has the lowest variance of RSS values in the radio map.

However, in real-life scenarios, i.e., large areas and multi-floor buildings, the Wi-Fi APs typically provide only partial coverage. Thus, the anchor AP could be different for those fingerprints collected in a part of the whole area based on the subset of Wi-Fi APs that are detected there. To this end, we define for any single device the SSD reference fingerprint $\check{\mathbf{r}}_i$

at reference location ℓ_i and the SSD fingerprint to be localized $\check{\mathbf{s}}$ as

$$\check{\mathbf{r}}_i = \{[\check{r}_{i1}, \ldots, \check{r}_{i(n-1)}]^\top, \rho_i\} \text{ and } \check{\mathbf{s}} = [\check{s}_1, \ldots, \check{s}_{n-1}]^\top, \quad (6)$$

where ρ_i denotes the anchor AP at location ℓ_i. The RSS differences between the j-th AP and the anchor AP in the reference and localization fingerprint are represented by

$$\check{r}_{ij} = r_{ij} - r_{i\rho_i} \text{ and } \check{s}_j = s_j - s_{\rho_i}, \quad (7)$$

where $j = 1, \ldots, n,\ j \neq \rho_i$. In the reference SSD fingerprint $\check{\mathbf{r}}_i$ we select ρ_i as the Wi-Fi AP that has the strongest RSS value in the original RSS fingerprint $\mathbf{r}_i$, as shown in Fig. 2. Note that the localization fingerprint $\check{\mathbf{s}}$ at the unknown location is recomputed online during localization based on the ρ_i in the reference fingerprint that is compared to.

Assuming M_i crowdsourcing devices at location ℓ_i, the differential radio map $\check{\mathbf{R}} \in \mathbb{Z}_{l\times(n-1)}$ contains the reference fingerprints $\check{\mathbf{r}}_i$ where $\check{r}_{ij}$ is computed using Eqn. (3) with $\check{r}_{ij}^{(m)}$, instead of $r_{ij}^{(m)}$. During positioning, the fingerprints $\check{\mathbf{r}}_i$ and $\check{\mathbf{s}}$ are used in Eqn. (4) to estimate the user location.

2) MDF Fingerprints: In the MDF method, the mean RSS value pertaining to all APs is subtracted from individual RSS values in the original fingerprint in order to create the differential fingerprints [27, 35]. As the Wi-Fi APs provide only partial coverage in large areas and multi-floor buildings, only a subset of the APs will be detected and provide valid RSS values in different parts. Figure 2 shows that a single device uses RSS collected from a subset of Wi-Fi APs to generate MDF fingerprints. Therefore, we define for a single device the MDF reference fingerprint $\bar{\bar{\mathbf{r}}}_i$ at reference location ℓ_i and the MDF fingerprint to be localized $\bar{\bar{\mathbf{s}}}$ as

$$\bar{\bar{\mathbf{r}}}_i = \{[\bar{\bar{r}}_{i1}, \ldots, \bar{\bar{r}}_{in}]^\top, \mathcal{A}_i\} \text{ and } \bar{\bar{\mathbf{s}}} = [\bar{\bar{s}}_1, \ldots, \bar{\bar{s}}_n]^\top, \quad (8)$$

where $\mathcal{A}_i$ denotes the subset of Wi-Fi APs that are detected at location ℓ_i. The RSS differences between the j-th AP and the mean RSS value in the reference and localization fingerprint are given by

$$\bar{\bar{r}}_{ij} = r_{ij} - \bar{r}_i \text{ and } \bar{\bar{s}}_j = s_j - \bar{s}, \quad (9)$$

$$\bar{r}_i = \frac{1}{|\mathcal{A}_i|}\sum_{j=1}^{|\mathcal{A}_i|} r_{ij} \text{ and } \bar{s} = \frac{1}{|\mathcal{A}_i|}\sum_{j=1}^{|\mathcal{A}_i|} s_j, \quad (10)$$

where $j = 1, \ldots, n$, and $|\mathcal{A}_i|$ denotes the number of Wi-Fi APs in subset $\mathcal{A}_i$. Note that the localization fingerprint $\bar{\bar{\mathbf{s}}}$, which is collected at an unknown location, is recomputed online during localization based on the $\mathcal{A}_i$ in the reference fingerprint that is compared to.

Assuming M_i crowdsourcing devices at location ℓ_i, the differential radio map $\bar{\bar{\mathbf{R}}} \in \mathbb{Z}_{l\times n}$ contains the reference fingerprints $\bar{\bar{\mathbf{r}}}_i$ where $\bar{\bar{r}}_{ij}$ is computed using Eqn. (3) with $\bar{\bar{r}}_{ij}^{(m)}$, instead of $r_{ij}^{(m)}$. Similarly to the SSD method, the MDF fingerprints $\bar{\bar{\mathbf{r}}}_i$ and $\bar{\bar{\mathbf{s}}}$ are used in Eqn. (4) for positioning.

Competitive advantages of MDF: In a nutshell, compared to other existing methods, MDF has the advantages of requiring less computation and having smaller noise variance in the measurements. Assuming that there are n Wi-Fi APs in the target area, the DIFF fingerprint contains all $\binom{n}{2}$ pairwise RSS differences. Thus, it is difficult to apply DIFF method where there are numerous APs. The SSD fingerprint contains $n-1$ RSS differences; however, selecting an anchor AP is not trivial in large-scale multi-floor indoor environments because the Wi-Fi APs provide only partial coverage. On the other hand, the MDF fingerprint contains n RSS differences, thus it keeps the fingerprint dimension low in contrast to the DIFF method. It was shown analytically in [27] that MDF achieves the same localization accuracy with DIFF (in fact it provides exactly the same estimated locations), but with significantly lower computational complexity due to the lower dimension of the MDF fingerprints. Importantly, it is easy to observe that the MDF measurements, by construction, have lower noise variance compared to the DIFF measurements, as well as the SSD measurements; see Eqn. (14) in Section III-A and Eqn. (30) in Appendix B. This implies that MDF is able to achieve better accuracy as demonstrated in the following example and the CRLB analysis in Section III-C.

3) Numerical Example of Differential Fingerprinting: A numerical example using RSS, MDF, and SSD in crowdsourced fingerprinting systems is shown in Table **??**. We assumed that two devices $D^{(1)}$ and $D^{(2)}$ with different characteristics collect RSS fingerprints from five Wi-Fi APs. Device $D^{(1)}$ is used to collect reference fingerprints for the radio maps, while $D^{(2)}$ collects the test fingerprints to be localized. For simplicity, we assumed that the parameters for mapping the heterogeneous RSS values between the two devices are $\alpha_{1,2} = 1, \gamma_{1,2} = -5$ [36]. The RSS test fingerprints are collected at the reference locations and are disturbed by adding a random integer in the range of $[-15, 15]$ dBm to the RSS values of the original reference fingerprints.

The RSS reference and test fingerprints at locations ℓ_1 and ℓ_2 are tabulated in Tables **??** and **??**. The corresponding SSD and MDF fingerprints are tabulated in Tables **??**, **??** and Tables **??**, and **??**, respectively. Columns 7 and 8 in Tables **??**, **??** and **??** show the distances d_1 and d_2 between the reference fingerprints and the test fingerprints. The location of the reference fingerprint that has the minimum distance from the test fingerprint is regarded as the estimated position, shown in the last column.

In this example, using the original RSS fingerprints results in performance degradation as the wrong location is computed for both test fingerprints. In contrast, differential fingerprinting methods perform better. Notably, the MDF method estimates the location correctly in both cases, while the SSD method provides the wrong location for the first test fingerprint.

III. Performance Analysis of MDF

In this section, we present the MDF measurement model and then derive the CRLB for the MDF method considering multiple devices. Finally, we apply the CRLB to analyze thoroughly the theoretical performance of MDF in crowdsourced fingerprinting systems.

A. MDF Measurement Model

Using Eqn. (1) and Eqn. (8), the MDF fingerprint measurement collected by device $D^{(m)}$ from the j-th Wi-Fi AP at the

reference location $\ell = [x, y]^\top$ can be obtained as[1],

$$\bar{\bar{r}}_j^{(m)} = -10\beta \log\left(\frac{d_j}{\prod_{j'=1}^{n} d_{j'}^{\frac{1}{n}}}\right) + X_{\text{MDF},j}^{(m)}, \quad (11)$$

where d_j is the distance between user's device and the j-th AP located at $[x_j, y_j]^\top$. The Gaussian noise of the MDF measurement from the j-th Wi-Fi AP is represented by:

$$X_{\text{MDF},j}^{(m)} = [X_j^{(m)} - (1/n)\sum_{j'=1}^{n} X_{j'}^{(m)}], \quad (12)$$

where $X_j^{(m)} \sim \mathcal{N}(0, (\sigma_j^{(m)})^2)$ is the Gaussian noise disturbing the Wi-Fi RSS measurement collected by device $D^{(m)}$.

Using Eqn. (3) and assuming for simplicity that $M_i = M,\ \forall i$, the MDF measurement $\bar{\bar{r}}_j$ across all crowdsourcing devices M follows a Gaussian distribution, $\bar{\bar{r}}_j \sim \mathcal{N}(\tilde{\mu}_j, \tilde{\sigma}_j^2)$, where $\tilde{\mu}_j$ and $\tilde{\sigma}_j^2$ are the mean and variance given by:

$$\tilde{\mu}_j = -10\beta \log\left(\frac{d_j}{\prod_{j'=1}^{n} d_{j'}^{\frac{1}{n}}}\right), \quad (13)$$

$$\tilde{\sigma}_j^2 = \frac{1}{M^2}\sum_{m=1}^{M}\left[\left(1 - \frac{2}{n}\right)(\sigma_j^{(m)})^2 + \frac{1}{n^2}\sum_{j'=1}^{n}(\sigma_{j'}^{(m)})^2\right], \quad (14)$$

where $\mathbb{E}[X_j^{(m)} X_{j'}^{(m)}] = 0$, $j \neq j'$ since $X_j^{(m)}$, $X_{j'}^{(m)}$ are independent noise measured by different Wi-Fi APs. The detailed derivations of the mean and variance are shown in Eqn. (20) and Eqn. (21) in Appendix A, respectively.

B. Derivation of the CRLB for MDF

The CRLB presents a lower bound on the variance of an unbiased estimator, which represents achievable estimator performance. With respect to indoor localization, the CRLB quantifies the lower bound of the localization error that can be achieved by any estimator at a specific position given indoor environmental factors. Here, we derive the CRLB of the user's location ℓ from the MDF measurements $\bar{\bar{\mathbf{r}}}$. If $\widehat{\ell} = [\widehat{x}, \widehat{y}]^\top$ is the estimate of the user's location, the CRLB of user's location is formulated by [37]:

$$\text{var}(\widehat{\ell}) \geq J(\ell)^{-1},\ J(\ell) = -\mathbb{E}\left\{\frac{\partial^2 \ln f(\bar{\bar{\mathbf{r}}}|\ell)}{\partial \ell^2}\right\}, \quad (15)$$

where $J(\ell)$ is the Fisher Information Matrix (FIM).

Theorem 1: The CRLB of the MDF method depends on i) the geometry of the Wi-Fi AP locations, ii) the distance between the Wi-Fi APs and the user device d_j, iii) the number of Wi-Fi APs n, iv) the number of crowdsourcing devices M, and v) the parameters of the propagation model β and σ. □

We prove Theorem 1 by deriving analytically the FIM $J(\ell)$. First, using the MDF measurement model for multiple crowdsourcing devices of Subsection III-A, the joint measurement likelihood function of the n MDF measurements is represented by the Gaussian distribution as follows:

$$f(\bar{\bar{\mathbf{r}}}|\ell) = \prod_{j=1}^{n} \frac{1}{\sqrt{2\pi}\tilde{\sigma}_j}\frac{10}{\ln 10}\frac{\bar{r}}{r_j}\times$$
$$\exp\left\{-\left[10\log\left(\frac{r_j}{\bar{r}}\right) + 10\beta\log\left(\frac{d_j}{\prod_{j'=1}^{n} d_{j'}^{\frac{1}{n}}}\right)\right]^2 \Big/ 2\tilde{\sigma}_j^2\right\}. \quad (16)$$

Let the FIM be denoted as

$$J(\ell) = \begin{bmatrix} J_{xx}(\ell) & J_{xy}(\ell) \\ J_{yx}(\ell) & J_{yy}(\ell) \end{bmatrix}, \quad (17)$$

while the entries of the FIM are given by:

$$\begin{aligned} J_{xx}(\ell) &= \sum_{j=1}^{n}\tilde{\kappa}_j\left[\Upsilon_j - \frac{1}{n}\sum_{j'=1}^{n}\Upsilon_{j'}\right]^2, \\ J_{xy}(\ell) &= J_{yx}(\ell) \\ &= \sum_{j=1}^{n}\tilde{\kappa}_j\left[\Upsilon_j - \frac{1}{n}\sum_{j'=1}^{n}\Upsilon_{j'}\right]\left[\Psi_j - \frac{1}{n}\sum_{j'=1}^{n}\Psi_{j'}\right], \\ J_{yy}(\ell) &= \sum_{j=1}^{n}\tilde{\kappa}_j\left[\Psi_j - \frac{1}{n}\sum_{j'=1}^{n}\Psi_{j'}\right]^2, \end{aligned} \quad (18)$$

where $\tilde{\kappa}_j = (10\beta/\tilde{\sigma}_j \ln 10)^2$, $\Upsilon_j = (x - x_j)/d_j^2$ and $\Psi_j = (y - y_j)/d_j^2$. The detailed derivation of the FIM entries are included in Appendix A. Since the diagonal elements of positive semidefinite matrices are larger or equal to zero, the CRLB of the MDF method is given by:

$$\text{var}(\widehat{\ell}) = \sigma_{\hat{x}}^2 + \sigma_{\hat{y}}^2 \geq \frac{J_{xx}(\ell) + J_{yy}(\ell)}{|J(\ell)|}. \quad (19)$$

Theorem 1 holds by observing the entries of the FIM in Eqn. (18). In particular, the geometry of the Wi-Fi APs is implicit in Υ_j and Ψ_j that contain the x and y coordinates of AP j and the user location respectively, as well as the distance d_j between the Wi-Fi APs and the user device. The number of the Wi-Fi APs n is also included in the FIM entries, while the number of crowdsourcing devices M and the propagation model parameters β and σ are included in the standard deviation of the MDF measurements $\tilde{\sigma}_j$.

C. CRLB Analysis of Fingerprinting Methods

We investigate the impact of previously identified factors on the localization performance of fingerprinting systems when the MDF and SSD are used in a simple localization setup. Heterogeneous devices collect Wi-Fi RSS measurements from 16 Wi-Fi APs marked in triangles that are placed at specified intervals, while the user-carried devices can be localized at the positions marked in circles [38], as shown in Fig. 3a. The associated simulation parameters for the CRLB computation are shown in Table **??**. Note that the dimensions of the localization setup vary accordingly with respect to the number of Wi-Fi APs and their pairwise distance, as listed in Table **??**.

[1]For brevity we drop the location index i. We also assume that all Wi-Fi APs cover the entire area of interest, thus we drop $\mathcal{A}_i$.

Similarly to the CRLB derivation for MDF, we derive the CRLB for SSD considering multiple heterogeneous devices; the details are provided in Appendix B. Note that we do not study explicitly the effect of the Wi-Fi AP geometry as the MDF follows the same trend reported for the RSS and SSD fingerprints (e.g., the worst-case configuration is when the APs are deployed along a line); see [34] and references therein for a discussion about the optimal placement of Wi-Fi APs in terms of localization accuracy. Note that the CRLB for the HLF and RBF methods are not derived, as it has been reported experimentally that they both attain lower localization accuracy compared to SSD and MDF [30].

1) Distance Between the Wi-Fi APs and the Device: The effect of the distance between Wi-Fi APs and the user's device on the CRLB is depicted in Fig. 3b. The values of the simulation parameters are shown in the second column of Table **??** and the distance between the Wi-Fi APs increases from $1\,\mathrm{m}$ to $10\,\mathrm{m}$ in $1\,\mathrm{m}$ intervals (i.e., the distance between each Wi-Fi AP and the device also increases). The values of the FIM entries in Eqn. (18) decrease as the distance between the Wi-Fi APs is increased; thus, the CRLB for all fingerprinting methods gets larger. This indicates that the localization accuracy degrades when the user's device is further from the Wi-Fi APs. However, we observe that the MDF provides better performance compared to the SSD fingerprints.

2) Number of Wi-Fi APs: The relationship between the number of Wi-Fi APs and the CRLB is illustrated in Fig. 3c. Starting with 3 Wi-Fi APs, more APs are added to the fingerprinting localization system according to their index number from 3 to 16, while the other parameters are shown in the third column of Table **??**. In this case, more information (i.e., RSS measurements) is available in the system to localize the user. Therefore, as the number of Wi-Fi APs increases, the FIM entries in Eqn. (18) get larger. Consequently, the CRLB of the fingerprinting methods decreases leading to higher localization accuracy with the MDF method performing better than SSD.

3) Number of Crowdsourcing Devices: We investigate the effect of the number of crowdsourcing devices on the CRLB of user's location using the parameters listed in the forth column of Table **??**. Each device has different characteristics that are represented by parameter A in Eqn. (1). We vary this parameter in $1\,\mathrm{dBm}$ increments from $-29\,\mathrm{dBm}$ to $-20\,\mathrm{dBm}$, while the number of devices increases accordingly. As shown in Fig. 3d, the tendency of the CRLB depends on the number of devices. When more devices are used for crowdsourcing, the variance of all differential fingerprints decreases. Thus, the values of the FIM entries in Eqn. (18) increase, resulting in lower CRLB value. Again, the MDF method outperforms the SSD method in terms of the CRLB and is capable to achieve better accuracy in multi-device crowdsourcing systems.

4) Impact of the Propagation Model Parameters: The impact of the two parameters in the propagation model Eqn. (1), i.e., the path-loss exponent and the standard deviation of the shadowing noise in the RSS measurements, is shown in Fig. 3e and Fig. 3f, respectively.

Fig. 3e shows the effect of path-loss exponent β on the CRLB. For β corresponding to various indoor environments, as the path-loss exponent β increases from 1.6 to 6, the CRLB decreases [39]. This implies that the localization accuracy is better in indoor environments, compared to outdoor environments. This is reasonable, as the challenging signal propagation conditions indoors increase the discriminate power of the RSS values (i.e., they are more likely to change significantly in short distances due to reflections, obstructions, etc.) compared to line-of-sight propagation outdoors. In any case, the MDF method achieves significantly lower CRLB.

Regarding the shadowing noise component, we consider three crowdsourcing devices whose RSS measurements are affected by noise with the same standard deviation σ that varies from $0.5\,\mathrm{dBm}$ to $10\,\mathrm{dBm}$. Looking at Fig. 3f, increasing σ leads to higher CRLB, i.e., lower localization accuracy should be expected. Again, this is reasonable because higher noise decreases the discriminate power of the RSS values (i.e., the RSS values at nearby locations do not change significantly over the noise threshold to reliably identify the location of the user). As the standard deviation σ of the RSS measurements increases, the variance of SSD measurements grows larger compared to MDF measurements; thus, the MDF fingerprints are more robust in real life applications.

parameter

IV. Experimental Evaluation

This section provides a comprehensive assessment of the localization accuracy attained by the fingerprinting methods in real-life setups. First, we introduce the datasets collected with multiple devices in two indoor environments. Then, we present the experimental results and discuss our observations, while considering the findings of the CRLB analysis.

A. Indoor Localization Datasets

Huawei Dataset: This small-scale dataset contains Wi-Fi RSS values collected with 8 devices in an area of $120\,\mathrm{m}\times40\,\mathrm{m}$ inside the Riemann Laboratory, Huawei Technologies, Xi'an, China. These devices include Honor V30, Huawei Mate20, Huawei Mate30, Xiaomi Mi8, Huawei P40, Google Pixel3, OPPO Ace2, Vivo iQOO Z1. Figure 4 shows the floor map of this typical office environment with Wi-Fi APs, reference positions and test positions where the fingerprints were collected. The floor map shows only some of the Wi-Fi APs, that are close to the reference and test positions.

The dataset contains 2,870,518 RSS measurements generated from Wi-Fi APs with 421 different Basic Service Set Identifiers (BSSID). Note that the number of APs is quite high because each AP is configured to have four virtual APs for network management purposes[2]. The Wi-Fi APs that are more frequently detected in the entire dataset (i.e., provide more measurements) are sorted in decreasing order and the RSS values corresponding to the top-400 Wi-Fi APs are used to create fingerprints. There are 65 reference locations and 7,275 reference fingerprints in total are collected by all devices to

[2]In practice, to accommodate the large number of Wi-Fi APs, one can apply AP selection techniques to reduce the dimension of the fingerprints and therefore the computational time during positioning (see Section 5 in [40]). Such techniques are beyond the scope of this work; however, we highlight that they are fully compatible with differential fingerprinting.

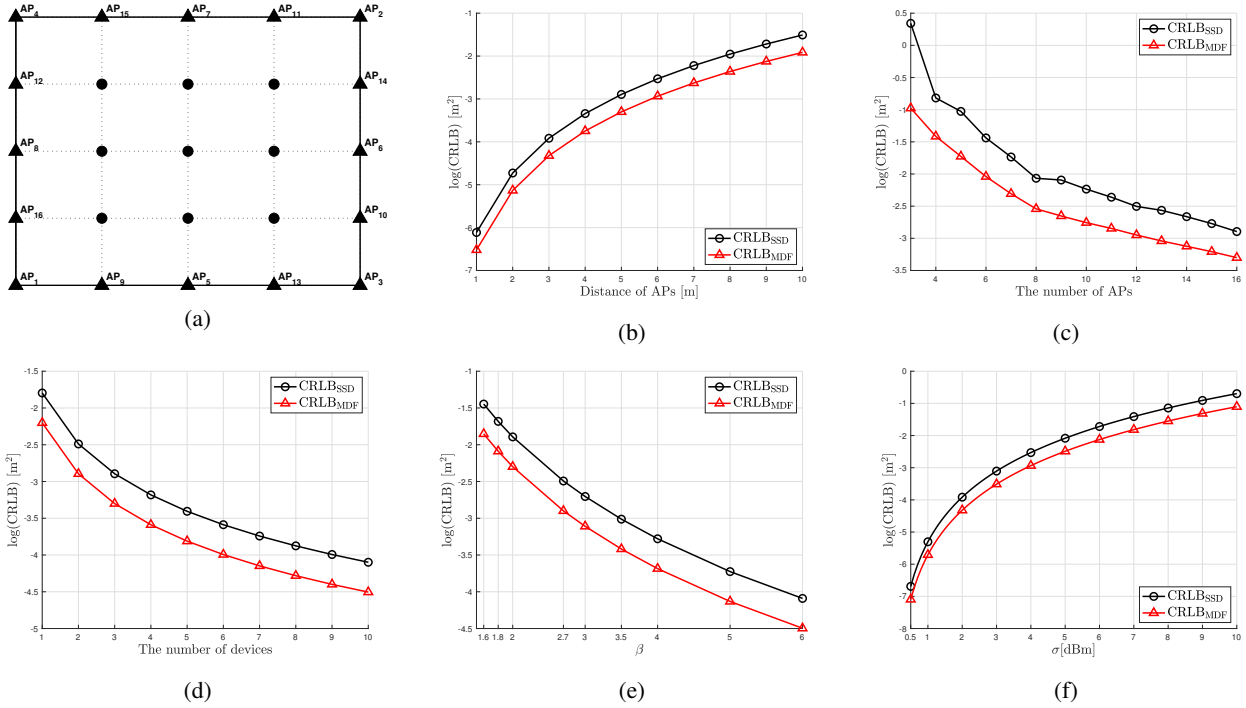

Fig. 3: (a) Localization setup for the CRLB analysis; CRLB versus the system parameter (b) distance between the Wi-Fi APs; (c) number of Wi-Fi APs; (d) number of crowdsourcing devices; (e) path-loss exponent; and (f) shadowing noise variance.

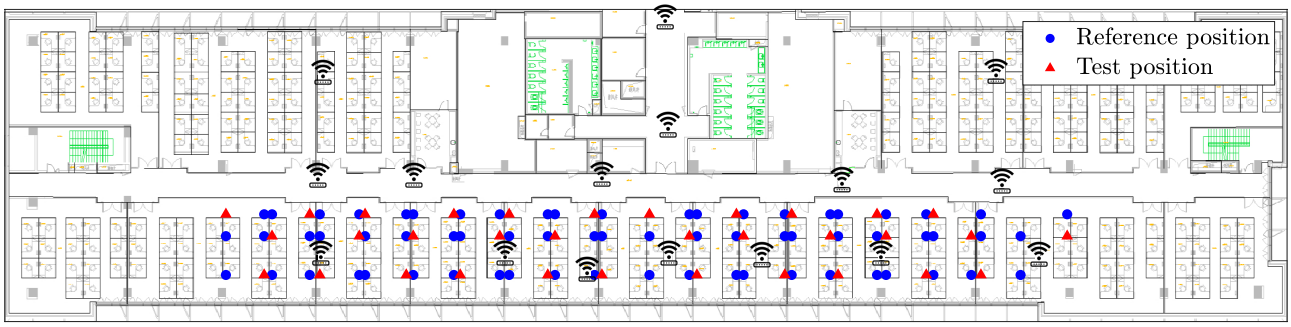

Fig. 4: Floor map of Huawei R&D office where Wi-Fi RSS fingerprints were collected.

build the crowdsourced radiomap. There are 33 test locations and 7,790 test fingerprints are collected by all devices, while the number of fingerprints collected by each device is different.

Tampere Dataset: This publicly available large-scale dataset contains 4,648 fingerprints collected by 21 devices in a five-floor university building in Tampere, Finland[3]. The building has a footprint of approximately $22.570\,\mathrm{m}^2$ (about $208\,\mathrm{m}$ length and $108\,\mathrm{m}$ width) [41]. This is a typical university building hosting a few larger lecture halls and several smaller lecture rooms on the first and second floor, as well as several offices and meeting rooms. The dataset contains 697 reference fingerprints and 3,951 test fingerprints. Each fingerprint contains RSS data from 992 Wi-Fi APs and we consider the top-600 APs with the largest volume of data.

[3]Tampere Dataset, https://doi.org/10.5281/zenodo.889798

B. Performance Metric & Results Reporting

We use these two datasets collected in real-life indoor environments to compare the MDF method against other solutions for crowdsourced fingerprinting localization, namely the standard RSS, the SSD [25], the HLF [23], and the RBF [22] methods. For the SSD method, the anchor AP is selected as described in Section II-B1. We followed the same approach for HLF to avoid the computational overhead of the original method that uses all pair-wise AP combinations.

We are interested in the accuracy of these methods in practice, thus we use the localization error as the performance metric that is defined as the Euclidean distance between the real user location and his/her location estimated by the K-NN localization approach given by Eqn. (4) using $K = 5$. We report statistics with respect to the distribution of the localization error using box plots and bar charts. The box plots

represent the empirical cumulative distribution function of the error where the central mark indicates the median error, the box edges correspond to the 25th and 75th percentiles, and the whiskers extend to the 5th and 95th percentiles, respectively. The bar charts present the mean localization error together with the 95% confidence interval given by $\pm 1.96\sigma_e/\sqrt{|T|}$, where σ_e is the standard deviation of the error and $|T|$ is the number of test samples. The 95% confidence interval indicates that the mean error falls within the interval with a high degree of certainty.

C. Experiments

In the following, we present the evaluation results and discuss our findings with respect to the localization error. We performed three series of experiments to investigate i) the combined effect of device heterogeneity and carrying mode in an office environment, ii) the additional effect of power control schemes in the Wi-Fi APs, and iii) the effect of device heterogeneity in larger indoor environments using several devices and sparsely collected data.

1) Effect of Device Heterogeneity and Carrying Mode: In this experiment, we investigate the combined impact of device heterogeneity and other factors on the RSS values that consequently affect the localization accuracy. We emulate such factors, e.g., various device carrying modes, by adding a different constant bias value to the RSS values reported by the 8 heterogeneous devices, i.e., from $0\,\mathrm{dBm}$ (no bias) for the Huawei Honor V30 to $-14\,\mathrm{dBm}$ for the Vivo iQOO Z1 in steps of $-2\,\mathrm{dBm}$ for the other devices.

We use 330 test fingerprints that the Huawei Honor V30 device collected, i.e., ten test fingerprints at each test location. Figure 5a shows the localization error achieved with this device considering all eight devices for crowdsourcing. The median localization error of MDF is about $2.36\,\mathrm{m}$, which is the lowest of the five fingerprinting methods.

The localization error for increasing number of crowdsourcing devices is illustrated in Fig. 5b. When $M = 1$, only the Honor V30 smartphone is used to build the radio map, and there is a difference of about $0.82\,\mathrm{m}$ in localization error between the RSS and MDF methods. As the number of devices increases, the localization performance for RSS fingerprints degrades because of the factors affecting the RSS values. We observe that the performance of the MDF method improves slightly as more crowdsourcing devices are considered.

2) Effect of Power Control in Wi-Fi APs: In this experiment, we focus on the localization error in the power control situation. It assumed that half of the Wi-Fi APs, which are randomly selected, perform power control. The power control offset is set to a random integer in the range of $[-3,\ 3]$ dBm. The fingerprints collected to build the radio map in the *offline* phase include the power control offset. In the *online* phase, the fingerprints have different offset because they were assumed to be collected in a different power control duration. Figure 5c illustrates the results of the mean localization error that are averaged over 5 Monte Carlo experiments for the increasing number of Wi-Fi APs. When there are 100 Wi-Fi APs, the localization error for all methods exceeds $3\,\mathrm{m}$. When $n = 200$, the localization error of MDF drops below $3\,\mathrm{m}$ and it outperforms other fingerprinting methods. As the number of APs increases, the performance of MDF improves further and then this effect gradually reduces, as shown in Fig. 3c.

3) Effect of Device Heterogeneity with Sparse Data From Several Devices: The localization error on the 2nd floor of the Tampere dataset, that includes 197 reference and 1,108 test fingerprints, is depicted in Fig. 5d. In this case, the median localization error of MDF is about $4\,\mathrm{m}$, which is well below other fingerprinting methods that achieve median error higher than $5\,\mathrm{m}$. In addition, the 25th and 75th percentile errors are the lowest compared to other methods.

Figure 5e shows the localization error for the increasing number of Wi-Fi APs by averaging over 5 Monte Carlo experiments with a different subset of Wi-Fi APs randomly selected in each experiment. As the number of Wi-Fi APs increases, the mean localization error of all fingerprinting methods decreases and the standard deviation of the localization error is reduced. The localization accuracy improves when more Wi-Fi APs are considered, while the MDF method achieves significantly better accuracy compared to other methods.

We observed the same trend using data from other floors. For instance, on the 3rd floor that contains 139 reference fingerprints and 770 test fingerprints MDF attains a median error of $5.01\,\mathrm{m}$ compared to $8.54\,\mathrm{m}$ for RSS and $7.28\,\mathrm{m}$ for SSD. Similarly, on the 4th floor (118 reference fingerprints and 699 test fingerprints) the median error of MDF is $3.98\,\mathrm{m}$ compared to $7.28\,\mathrm{m}$ for RSS and $5.55\,\mathrm{m}$ for SSD.

V. Conclusions

Differential fingerprinting methods are able to address the challenges in crowdsourced IPSs raised by various factors that affect the RSS measurements such as device heterogeneity, device carrying mode, and power control of Wi-Fi APs. In this work, we use a methodology based on the CRLB to show analytically that the MDF method is preferable for building the fingerprints, instead of the original RSS fingerprints, as it provides measurements that are more robust to these factors. Extensive experimental results with real-life data confirm our analytical findings and demonstrate that the MDF method handles effectively the RSS measurements provided by multiple devices and delivers higher accuracy, compared to existing solutions.

As part of our future work we plan to incorporate the MDF method in production-level IPSs such as the Anyplace Navigation Service[4] developed at the University of Cyprus to improve user experience when navigating in indoor environments.

[4] Anyplace Navigation Service, https://anyplace.cs.ucy.ac.cy/

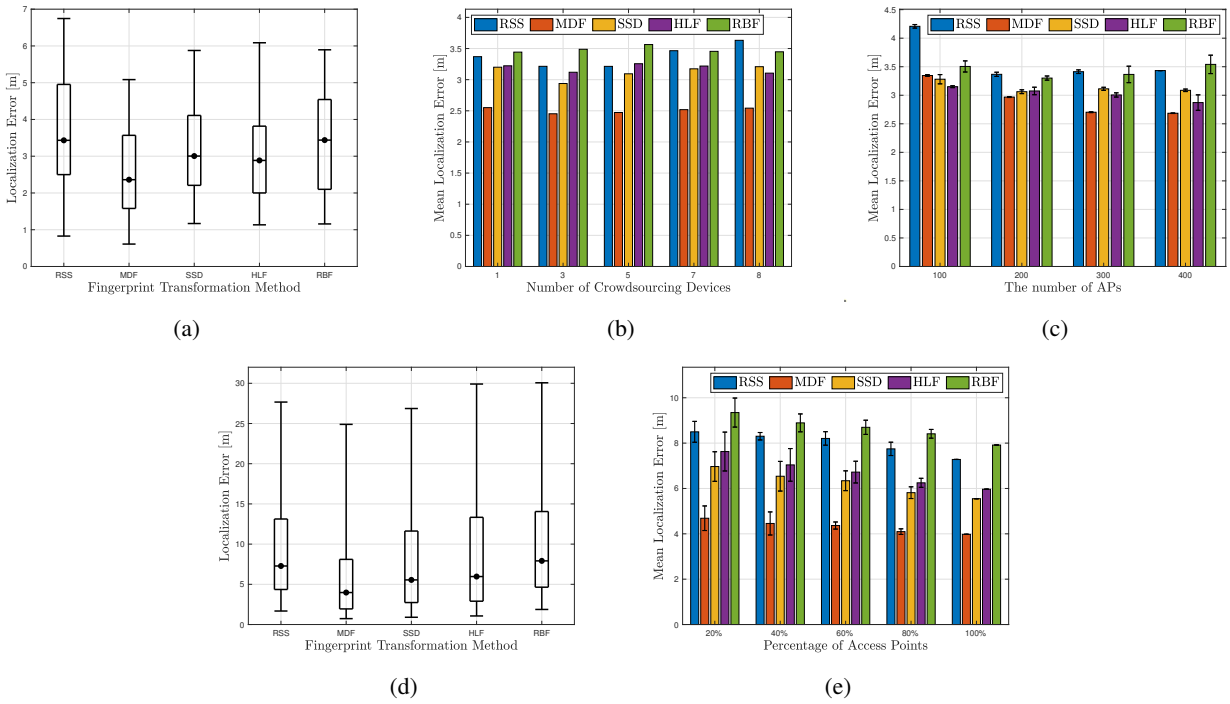

Fig. 5: Localization of the Honor V30 device (a) with crowdsourced data from all 8 devices; (b) for increasing number of crowdsourcing devices; (c) in the power control situation; Localization results on the 2nd floor of the Tampere dataset (d) with crowdsourced data from all 21 devices; and (e) for the increasing number of Wi-Fi APs.

Appendix A
CRLB derivation for the MDF method

The details of the CRLB derivation are described here. The mean and variance of MDF are calculated as follows:

$$\begin{aligned}\tilde{\mu}_j &= \mathbb{E}\left[\frac{1}{M}\sum_{m=1}^{M}\bar{\bar{r}}_j^{(m)}\right] \\ &= \frac{1}{M}\sum_{m=1}^{M}\mathbb{E}\left[-10\beta\log\left(\frac{d_j}{\prod_{j'=1}^{n} d_{j'}^{\frac{1}{n}}}\right)+X_{\text{MDF},j}^{(m)}\right] \\ &= -10\beta\log\left(\frac{d_j}{\prod_{j'=1}^{n} d_{j'}^{\frac{1}{n}}}\right),\end{aligned} \tag{20}$$

$$\begin{aligned}\tilde{\sigma}_j^2 &= \mathbb{E}\left[(\bar{\bar{r}}_j-\tilde{\mu}_j)^2\right] \\ &= \mathbb{E}\left[\left\{\frac{1}{M}\sum_{m=1}^{M}\left(X_j^{(m)}-\frac{1}{n}\sum_{j'=1}^{n}X_{j'}^{(m)}\right)\right\}^2\right] \\ &= \frac{1}{M^2}\sum_{m=1}^{M}\left[\left(1-\frac{2}{n}\right)(\sigma_j^{(m)})^2+\frac{1}{n^2}\sum_{j'=1}^{n}(\sigma_{j'}^{(m)})^2\right],\end{aligned} \tag{21}$$

The log-likelihood of Eqn. (16) can be represented by:

$$\ln f(\bar{\bar{\mathbf{r}}}|\ell)=\sum_{j=1}^{n}\left[\ln\frac{1}{\sqrt{2\pi}\tilde{\sigma}_j}\frac{10}{\ln 10}\frac{\bar{r}}{r_j}-\frac{\tilde{\kappa}_j}{8}\left(\ln\frac{d_j^2}{\tilde{d}_j^2}\right)^2\right], \tag{22}$$

where $\tilde{\kappa}_j=(10\beta/\tilde{\sigma}_j\ln 10)^2$ and $\tilde{d}_j=(\bar{r}/r_j)^{1/\beta}\prod_{j'=1}^{n}d_{j'}^{1/n}$. The derivatives of $\ln f(\bar{\bar{\mathbf{r}}}|\ell)$ with respect to each coordinate are as follows:

$$\frac{\partial}{\partial x}\ln f(\bar{\bar{\mathbf{r}}}|\ell)=\sum_{j=1}^{n}\left[-\frac{\tilde{\kappa}_j}{2}\ln\frac{d_j^2}{\tilde{d}_j^2}\left(\Upsilon_j-\frac{1}{n}\sum_{j'=1}^{n}\Upsilon_{j'}\right)\right], \tag{23}$$

$$\frac{\partial}{\partial y}\ln f(\bar{\bar{\mathbf{r}}}|\ell)=\sum_{j=1}^{n}\left[-\frac{\tilde{\kappa}_j}{2}\ln\frac{d_j^2}{\tilde{d}_j^2}\left(\Psi_j-\frac{1}{n}\sum_{j'=1}^{n}\Psi_{j'}\right)\right], \tag{24}$$

where $\Upsilon_j=(x-x_j)/d_j^2$ and $\Psi_j=(y-y_j)/d_j^2$. In order to calculate the entries of FIM, we obtain the following equations by taking the derivative of Eqn. (23) and Eqn. (24) w.r.t. ℓ:

$$\begin{aligned}\frac{\partial^2}{\partial x^2}\ln f(\bar{\bar{\mathbf{r}}}|\ell)=\sum_{j=1}^{n}-\frac{\tilde{\kappa}_j}{2}\Bigg[&2\left(\Upsilon_j-\frac{1}{n}\sum_{j'=1}^{n}\Upsilon_{j'}\right)^2 \\ &+\left(\ln\frac{d_j^2}{\tilde{d}_j^2}\right)\frac{\partial}{\partial x}\left(\Upsilon_j-\frac{1}{n}\sum_{j'=1}^{n}\Upsilon_{j'}\right)\Bigg],\end{aligned} \tag{25}$$

$$\frac{\partial^2}{\partial x \partial y} \ln f(\bar{\tilde{\mathbf{r}}}|\ell) = \frac{\partial^2}{\partial y \partial x} \ln f(\bar{\tilde{\mathbf{r}}}|\ell)$$
$$= \sum_{j=1}^{n} -\frac{\tilde{\kappa}_j}{2} \left[2 \left(\Upsilon_j - \frac{1}{n} \sum_{j'=1}^{n} \Upsilon_{j'} \right) \left(\Psi_j - \frac{1}{n} \sum_{j'=1}^{n} \Psi_{j'} \right) + \left(\ln \frac{d_j^2}{\tilde{d}_j^2} \right) \frac{\partial}{\partial y} \left(\Upsilon_j - \frac{1}{n} \sum_{j'=1}^{n} \Upsilon_{j'} \right) \right], \tag{26}$$

$$\frac{\partial^2}{\partial y^2} \ln f(\bar{\tilde{\mathbf{r}}}|\ell) = \sum_{j=1}^{n} -\frac{\tilde{\kappa}_j}{2} \left[2 \left(\Psi_j - \frac{1}{n} \sum_{j'=1}^{n} \Psi_{j'} \right)^2 + \left(\ln \frac{d_j^2}{\tilde{d}_j^2} \right) \frac{\partial}{\partial y} \left(\Psi_j - \frac{1}{n} \sum_{j'=1}^{n} \Psi_{j'} \right) \right]. \tag{27}$$

All of the second derivatives of the log-likelihood include a term of $\ln(d_j^2/\tilde{d}_j^2)$ whose expected value is zero.

Appendix B
CRLB derivation for the SSD method

Without loss of generality, we assume a single Wi-Fi AP used as the anchor AP, i.e., $\rho_i = k$, at all locations ℓ_i and all crowdsourcing devices M. The SSD measurement from the j-th Wi-Fi AP for device $D^{(m)}$ is represented by:

$$\check{r}_j^{(m)} = -10\beta \log \left(\frac{d_j}{d_k} \right) + X_{\text{SSD},j}^{(m)}, \tag{28}$$

where $X_{\text{SSD},j}^{(m)} = [X_j^{(m)} - X_k^{(m)}]$ is the shadowing noise of the SSD measurement. In the same way presented in Section III-A, the mean and variance of the SSD measurement are obtained by:

$$\check{\mu}_j = \mathbb{E}\left[\frac{1}{M} \sum_{m=1}^{M} \check{r}_j^{(m)} \right] = \frac{1}{M} \sum_{m=1}^{M} \mathbb{E}\left[-10\beta \log \left(\frac{d_j}{d_k} \right) + X_{\text{SSD},j}^{(m)} \right] = -10\beta \log \left(\frac{d_j}{d_k} \right), \tag{29}$$

$$\check{\sigma}_j^2 = \mathbb{E}\left[(\check{r}_j - \check{\mu}_j)^2 \right] = \mathbb{E}\left[\left\{ \frac{1}{M} \sum_{m=1}^{M} \left(X_j^{(m)} - X_k^{(m)} \right) \right\}^2 \right] = \frac{1}{M^2} \sum_{m=1}^{M} \left[(\sigma_j^{(m)})^2 + (\sigma_k^{(m)})^2 \right]. \tag{30}$$

The measurement likelihood function is given by:

$$f(\check{\mathbf{r}}|\ell) = \prod_{j=1}^{n-1} \frac{1}{\sqrt{2\pi}\check{\sigma}_j} \frac{10}{\ln 10} \frac{r_k}{r_j} \times \exp \left\{ -\left[10 \log \left(\frac{r_j}{r_k} \right) + 10\beta \log \left(\frac{d_j}{d_k} \right) \right]^2 \Big/ 2\check{\sigma}_j^2 \right\}. \tag{31}$$

The entries of the FIM given by Eqn. (15) are as follows:

$$J_{xx}(\ell) = \sum_{j=1}^{n-1} \check{\kappa}_j \left[\Upsilon_j - \Upsilon_k \right]^2, \; J_{yy}(\ell) = \sum_{j=1}^{n-1} \check{\kappa}_j \left[\Psi_j - \Psi_k \right]^2,$$
$$J_{xy}(\ell) = J_{yx}(\ell) = \sum_{j=1}^{n-1} \check{\kappa}_j \left[\Upsilon_j - \Upsilon_k \right] \left[\Psi_j - \Psi_k \right], \tag{32}$$

where $\check{\kappa}_j = (10\beta/\check{\sigma}_j \ln 10)^2$, $\Upsilon_j = (x - x_j)/d_j^2$ and $\Psi_j = (y - y_j)/d_j^2$.

Appendix C
Measurement Model of RSS Fingerprints

The RSS fingerprint collected by device $D^{(m)}$ from the j-th Wi-Fi AP is given by:

$$r_j^{(m)} = A^{(m)} - 10\beta \log(d_j) + X_j^{(m)}. \tag{33}$$

Regarding the original RSS measurement r_j, the mean and variance across all crowdsourcing devices M are obtained by:

$$\mu_j = \frac{1}{M} \sum_{m=1}^{M} A^{(m)} - 10\beta \log d_j, \tag{34}$$

$$\sigma_j^2 = \frac{1}{M^2} \sum_{m=1}^{M} (\sigma_j^m)^2. \tag{35}$$

Observing the mean, it is obvious that the RSS measurement is not robust to device heterogeneity as it contains the device dependent terms $A^{(m)}$.

References

[1] K. W. Kolodziej and J. Hjelm, *Local positioning systems: LBS applications and services*. CRC press, 2017.

[2] M. Mercuri, G. Sacco, R. Hornung, P. Zhang, H. J. Visser, M. Hijdra, Y.-H. Liu, S. Pisa, B. van Liempd, and T. Torfs, "2-D localization, angular separation and vital signs monitoring using a SISO FMCW radar for smart long-term health monitoring environments," *IEEE Internet Things J.*, vol. 8, no. 14, pp. 11 065–11 077, 2021.

[3] G. Paolini, D. Masotti, F. Antoniazzi, T. Salmon Cinotti, and A. Costanzo, "Fall detection and 3-D indoor localization by a custom RFID reader embedded in a smart e-health platform," *IEEE Trans. Microw. Theory Tech.*, vol. 67, no. 12, pp. 5329–5339, 2019.

[4] J. Rezazadeh, K. Sandrasegaran, and X. Kong, "A location-based smart shopping system with IoT technology," in *Proc. IEEE World Forum Internet Things (WF-IoT)*, 2018, pp. 748–753.

[5] S. Kuutti, S. Fallah, K. Katsaros, M. Dianati, F. Mccullough, and A. Mouzakitis, "A survey of the state-of-the-art localization techniques and their potentials for autonomous vehicle applications," *IEEE Internet Things J.*, vol. 5, no. 2, pp. 829–846, 2018.

[6] M. Mohammadi, A. Al-Fuqaha, M. Guizani, and J. Oh, "Semisupervised deep reinforcement learning in support of IoT and smart city services," *IEEE Internet Things J.*, vol. 5, no. 2, pp. 624–635, 2018.

[7] B. Hofmann-Wellenhof, H. Lichtenegger, and J. Collins, *Global positioning system: theory and practice*. Springer Science & Business Media, 2012.

[8] C. Yang and H.-r. Shao, "WiFi-based indoor positioning," *IEEE Commun. Mag.*, vol. 53, no. 3, pp. 150–157, 2015.

[9] K. Song, X. Liu, and T. Gao, "Potential application of using smartphone sensor for estimating air temperature: Experimental study," *IEEE Internet Things J.*, pp. 1–1, 2021.

[10] J. Hu, D. Liu, Z. Yan, and H. Liu, "Experimental Analysis on Weight K-Nearest Neighbor Indoor Fingerprint Positioning," *IEEE Internet Things J.*, vol. 6, no. 1, pp. 891–897, 2019.

[11] C.-Y. Chen, A. I.-C. Lai, P.-Y. Wu, and R.-B. Wu, "Optimization and Evaluation of Multi-Detector Deep Neural Network for High Accuracy Wi-Fi Fingerprint Positioning," *IEEE Internet Things J.*, pp. 1–1, 2022.

[12] G. Huang, Z. Hu, J. Wu, H. Xiao, and F. Zhang, "WiFi and Vision-Integrated Fingerprint for Smartphone-Based Self-Localization in Public Indoor Scenes," *IEEE Internet Things J.*, vol. 7, no. 8, pp. 6748–6761, 2020.

[13] C. Laoudias, A. Moreira, S. Kim, S. Lee, L. Wirola, and C. Fischione, "A survey of enabling technologies for network localization, tracking, and navigation," *IEEE Commun. Surveys Tuts.*, vol. 20, no. 4, pp. 3607–3644, 2018.

[14] R. Guan and R. Harle, "Towards a crowdsourced radio map for indoor positioning system," in *Proc. IEEE Int. Conf. Pervasive Comput. Commun. Workshops (PerCom)*, 2017, pp. 207–212.

[15] B. Wang, Q. Chen, L. T. Yang, and H.-C. Chao, "Indoor smartphone localization via fingerprint crowdsourcing: Challenges and approaches," *IEEE Wireless Commun.*, vol. 23, no. 3, pp. 82–89, 2016.

[16] G. Chatzimilioudis, A. Konstantinidis, C. Laoudias, and D. Zeinalipour-Yazti, "Crowdsourcing with smartphones," *IEEE Internet Comput.*, vol. 16, no. 5, pp. 36–44, 2012.

[17] F. D. Rosa, L. Xu, J. Nurmi, C. Laoudias, M. Pelosi, and A. Terrezza, "Hand-grip and body-loss impact on rss measurements for localization of mass market devices," in *Int. Conf. Localization and GNSS (ICL-GNSS)*, 2011, pp. 58–63.

[18] S.-Y. Lin, F.-Y. Leu, C.-Y. Ko, and M.-C. Shih, "A deep learning-based indoor-positioning approach using received strength signal indication and carrying mode information," *Concurrency and Computation: Practice and Experience*, no. cpe.6135, 2020.

[19] P. Bahl, M. T. Hajiaghayi, K. Jain, S. V. Mirrokni, L. Qiu, and A. Saberi, "Cell breathing in Wireless LANs: Algorithms and evaluation," *IEEE Trans. Mobile Comput.*, vol. 6, no. 2, pp. 164–178, Feb. 2007.

[20] "Huawei AP4050DN Access Point," Datasheet. [Online]. Available: https://bit.ly/3vYXLBA

[21] J. Ledlie, J. Park, D. Curtis, A. Cavalcante, L. Camara, A. Costa, and R. Vieira, "Molé: a scalable, user-generated WiFi positioning engine," *J. Location Based Services*, vol. 6, no. 2, pp. 55–80, Jun. 2012.

[22] S. Yang, P. Dessai, M. Verma, and M. Gerla, "FreeLoc: Calibration-free crowdsourced indoor localization," in *Proc. IEEE Int. Conf. Comput. Commun. (INFOCOM)*, 2013, pp. 2481–2489.

[23] M. B. Kjærgaard, "Indoor location fingerprinting with heterogeneous clients," *Pervasive Mobile Comput.*, vol. 7, no. 1, pp. 31–43, 2011.

[24] F. Dong, Y. Chen, J. Liu, Q. Ning, and S. Piao, "A calibration-free localization solution for handling signal strength variance," in *Proc. 2nd Int. Conf. Mobile Entity Localization and Tracking in GPS-less environments (MELT)*, 2009, pp. 79–90.

[25] A. Mahtab Hossain, Y. Jin, W.-S. Soh, and H. N. Van, "SSD: A robust RF location fingerprint addressing mobile devices' heterogeneity," *IEEE Trans. Mobile Comput.*, vol. 12, no. 1, pp. 65–77, 2013.

[26] C. Laoudias, D. Zeinalipour-Yazti, and C. G. Panayiotou, "Crowdsourced indoor localization for diverse devices through radiomap fusion," in *Proc. IEEE Int. Conf. Indoor Positioning Indoor Navigation (IPIN)*. IEEE, 2013, pp. 1–7.

[27] C. Laoudias, P. Kolios, and C. Panayiotou, "Differential signal strength fingerprinting revisited," in *Proc. Int. Conf. Indoor Positioning Indoor Navigation (IPIN)*, 2014, pp. 30–37.

[28] S.-I. Sou, W.-H. Lin, K.-C. Lan, and C.-S. Lin, "Indoor location learning over wireless fingerprinting system with particle markov chain model," *IEEE Access*, vol. 7, pp. 8713–8725, 2019.

[29] X. Guo, L. Li, N. Ansari, and B. Liao, "Accurate WiFi Localization by Fusing a Group of Fingerprints via a Global Fusion Profile," *IEEE Trans. Veh. Technol.*, vol. 67, no. 8, pp. 7314–7325, 2018.

[30] C. Laoudias, S. Kim, D. Zeinalipour-Yazti, and C. G. Panayiotou, "A qualitative and quantitative evaluation of differential signal strength fingerprinting methods," in *IEEE Int. Conf. Commun. (ICC)*, May 2019, pp. 1–6.

[31] F. Gustafsson and F. Gunnarsson, "Mobile positioning using wireless networks: possibilities and fundamental limitations based on available wireless network measurements," *IEEE Signal Process. Mag.*, vol. 22, no. 4, pp. 41–53, 2005.

[32] A. Haeberlen, E. Flannery, A. M. Ladd, A. Rudys, D. S. Wallach, and L. E. Kavraki, "Practical robust localization over large-scale 802.11 wireless networks," in *Proc. Int. Conf. Mobile Comput. Netw.* ACM, 2004, p. 7084.

[33] J. Park, D. Curtis, S. Teller, and J. Ledlie, "Implications of device diversity for organic localization," in *Proc. IEEE Int. Conf. Comput. Commun. (INFOCOM)*, 2011, pp. 3182–3190.

[34] A. Hossain and W.-S. Soh, "Cramer-Rao bound analysis of localization using signal strength difference as location fingerprint," in *Proc. IEEE Int. Conf. Comput. Commun. (INFOCOM)*, 2010, pp. 1–9.

[35] C. Laoudias, "Localization and tracking in wireless networks for fault tolerance and device diversity," Ph.D. dissertation, University of Cyprus, Faculty of Engineering, May 2014. [Online]. Available: https://gnosis.library.ucy.ac.cy/handle/7/39260

[36] C. Laoudias, D. Zeinalipour-Yazti, and C. G. Panayiotou, "Crowdsourced indoor localization for diverse devices through radiomap fusion," in *Int. Conf. Indoor Positioning Indoor Navigation (IPIN)*, 2013, pp. 1–7.

[37] Y. Bar-Shalom, X. R. Li, and T. Kirubarajan, *Estimation with applications to tracking and navigation: theory algorithms and software*. John Wiley & Sons, 2004.

[38] K. Kaemarungsi and P. Krishnamurthy, "Modeling of indoor positioning systems based on location fingerprinting," in *Proc. IEEE Int. Conf. Comput. Commun. (INFOCOM)*, vol. 2, 2004, pp. 1012–1022.

[39] J. Miranda, R. Abrishambaf, T. Gomes, P. Gonalves, J. Cabral, A. Tavares, and J. Monteiro, "Path loss exponent analysis in wireless sensor networks: Experimental evaluation," in *2013 11th IEEE Int. Conf. Ind. Informat. (INDIN)*, 2013, pp. 54–58.

[40] A. Kushki, K. N. Plataniotis, and A. N. Venetsanopoulos, "Kernel-based positioning in wireless local area networks," *IEEE Trans. Mobile Comput.*, vol. 6, no. 6, pp. 689–705, 2007.

[41] E. S. Lohan, J. Torres-Sospedra, H. Leppkoski, P. Richter, Z. Peng, and J. Huerta, "Wi-Fi crowdsourced fingerprinting dataset for indoor positioning," *Data*, vol. 2, no. 4, 2017.

Jiseon Moon received her B.S. degree in Information Communication Engineering from Inha University of Incheon, South Korea, in 2019. She is currently pursuing the combined masters and Ph.D. degrees in the Department of Electronics and Computer Engineering from Hanyang University, Seoul, South Korea. Her research interests include wireless localization/positioning systems, multi-target tracking and location-aware communications

Laoudias.jpg

Christos Laoudias is a Research Lecturer at KIOS Research and Innovation Center of Excellence (CoE), University of Cyprus leading various projects and activities related to localization, tracking, and navigation in wireless networks. Before that he was leading the geolocation technology group in Huawei Ireland Research Center. He holds a Diploma in Computer Engineering and Informatics (2003) and a M.Sc. in Integrated Hardware and Software Systems (2005) from the University of Patras, Greece, and a Ph.D. in Computer Engineering from the University of Cyprus (2014). His research interests include positioning and tracking technologies, mobile and pervasive location-awareness, fault-tolerant location estimation, and location-based services.

Ran Guan received his BEng degrees from the University of Edinburgh, UK and the South China University of Technology, China, in 2014, and his M.Phil. and Ph.D. degrees in 2015 and 2020 from the University of Cambridge, UK. He currently works at the Riemann Laboratory, Huawei Technologies.

Sunwoo Kim (S'99-M'05-SM'17) received his B.S degree from Hanyang University, Seoul, Korea in 1999, and his Ph.D. degree, in 2005, from the Department of Electrical and Computer Engineering, University of California, Santa Barbara. Since 2005, he has been working in the Department of Electronic Engineering at Hanyang University, Seoul, Korea, where he is currently a professor. He is also the director of the 5G/Unmanned Vehicle Research Center, funded by the Ministry of Science and ICT of Korea. He was a visiting scholar to the Laboratory for Information and Decision Systems, Massachusetts Institute of Technology from 2018 to 2019. He is an associate editor of IEEE Transactions on Vehicular Technology. He is a senior member of the IEEE. His research interests include wireless communication/positioning/localization, signal processing, vehicular networks, and location-aware communications.

Demetrios Zeinalipour-Yazti is an Associate Professor of Computer Science at the University of Cyprus, where he directs the Data Management Systems Laboratory (DMSL). He holds a Ph.D. (2005) and an M.Sc. (2003) in Computer Science and Engineering from the University of California - Riverside, CA, USA and a B.Sc. in Computer Science from the University of Cyprus (2000). He has held short-term research visits at Akamai Technologies, Cambridge, MA, USA (2004), the University of Athens, Greece (2007) as a Marie-Curie Fellow and the University of Pittsburgh, PA, USA (2015). During 2016-2017, he was a Humboldt Fellow at the Max Planck Institute for Informatics, Saarbrcken, Germany. He is an ACM Distinguished Speaker (2017-2020), a Senior Member of ACM and a Senior Member of IEEE. His research interests include Data Management in Computer Systems and Networks.

Christos G. Panayiotou is a Professor with the ECE Department at the University of Cyprus and the Deputy Director of the KIOS Research and Innovation Center of Excellence. He holds B.Sc. (1994), Ph.D. (1999), and MBA (1999) degrees from the University of Massachusetts at Amherst. His research focuses on performance evaluation and optimization of intelligent transportation systems, modeling and control of discrete event and hybrid systems, cyber-physical systems, IoT, smart buildings, fault diagnosis, event detection and localization.